CellPress

Review

Neural Cross-Frequency Coupling: Connecting Architectures, Mechanisms, and Functions

Alexandre Hyafil,[1,2,*] Anne-Lise Giraud,[3] Lorenzo Fontolan,[3] and Boris Gutkin[4,5]

Neural oscillations are ubiquitously observed in the mammalian brain, but it has proven difficult to tie oscillatory patterns to specific cognitive operations. Notably, the coupling between neural oscillations at different timescales has recently received much attention, both from experimentalists and theoreticians. We review the mechanisms underlying various forms of this cross-frequency coupling. We show that different types of neural oscillators and cross-frequency interactions yield distinct signatures in neural dynamics. Finally, we associate these mechanisms with several putative functions of cross-frequency coupling, including neural representations of multiple environmental items, communication over distant areas, internal clocking of neural processes, and modulation of neural processing based on temporal predictions.

Mechanistic and Functional Characteristics of Cross-Frequency Coupling

Brain oscillations are observed *in vivo* and *in vitro* in almost any neuronal population of the neo- and paleocortex. While it is relatively easy to measure oscillations and observe their modulations in various sensory states and cognitive operations, it remains largely unclear what role, if any, they play in neural information processing or, more generally, in cognition [1,2]. An intriguing feature of neural oscillations is that rhythms of distinct frequencies show specific coupling properties [3–5]. The best-studied example of **cross-frequency coupling** (CFC, see Glossary) is between theta (4–8 Hz) and gamma (>30 Hz) oscillatory activity in the rodent hippocampus [5–7]. Several other observations of CFC, reported in a variety of species, brain regions, experimental conditions, and recording techniques, have been linked to distinct cognitive processes [7–10], but the functional significance of CFC remains enigmatic and its neuronal substrate obscure. The current working hypothesis is that different functions ascribed to CFC, including the representation of multiple items [7,11], communication between distant areas [12], and parsing of sensory stimuli with complex temporal structure [8], could arise from specific CFC patterns.

To clarify the potential roles of CFC, mechanistic and functional levels of description need to be brought together. These two strands of research have so far largely grown independently. To wit, functional models of CFC generally elude committing to precise underlying neural mechanisms, and dynamical models of CFC typically do not generate specific predictions about CFC signatures and related functions. The goal of this review is to draw a closer link between CFC mechanisms and functions. First, we introduce a novel classification of CFC phenomena according to the underlying architectures: whether they are generated by intermingled or by independent neuronal circuits, and whether the ensuing cross-frequency modulation is weak or

Trends

Cross-frequency coupling (CFC), in other words the association of multiple frequency neural oscillations, is present across different frequency bands and neural systems.

Circuit mechanisms determine CFC characteristics: oscillations generated in distinct versus overlapping circuits, and continuously active versus intermittent fast oscillation (FO).

Dynamic network properties determine CFC signatures: phase–phase coupling occur under weakly coupling and do not co-occur with phase–frequency coupling; phase–amplitude coupling is present when the FO is intermittent or sparse spiking; amplitude–amplitude coupling requires asymmetrical slow oscillations.

CFC is mechanistically implicated in three cognitive operations: multi-item representation, long-distance communication, and stimulus parsing.

Modeling shows that theta–gamma CFC is an intracortical mechanism for parsing speech.

[1]Universitat Pompeu Fabra, Theoretical and Computational Neuroscience, Roc Boronat 138, 08018 Barcelona, Spain
[2]Research Unit, Parc Sanitari Sant Joan de Déu and Universitat de Barcelona, Esplugues de Llobregat, Barcelona, Spain

© 2015 Elsevier Ltd. All rights reserved.

strong. We then relate each architecture to an existing computational model, and connect the various CFC signatures to specific neural mechanisms. Finally, we address how such neural mechanisms may specifically underpin the commonly proposed CFC functions. Our novel framework allows us to go beyond describing the various CFC phenomena because it lays down a conceptual scaffold for the distinct CFC signatures as experimental markers of specific neural mechanisms and cognitive functions.

CFC Architectures and Mechanisms

The first requirement for a network to generate CFC is to produce neural oscillations at two distinct frequencies. Three elementary architectures allow neuronal circuits to synchronize spiking activity and generate periodic rhythms: (i) synaptic coupling between inhibitory neurons, (ii) synaptic coupling across inhibitory and excitatory neurons, and (iii) electrical coupling via gap junctions – see [1]. When synaptic coupling generates synchrony, the decay time of inhibition is a major determinant of the oscillation frequency [13]. Subpopulations of interneurons, with slower and faster synaptic dynamics, as found in both the hippocampus and the neocortex [6,14], can give rise to coupled neural oscillations at distinct frequencies. We focus here exclusively on CFC between two neural oscillations that we refer to as fast and slow oscillations, abbreviated FO and SO, respectively.

The second requirement for a neural network to produce CFC lies in the coupling between the neural circuits that generate the individual oscillations. Depending on the nature of the coupling different CFC classes can be distinguished. Intermingled CFC networks (Figure 1A) refer to architectures where circuits generating individual oscillations share a common subpopulation, while independent CFC networks refer to separate populations generating the two oscillations. This case further divides into two subtypes: bidirectional coupling (Figure 1B), where two reciprocally coupled populations generate individual oscillations, and unidirectional coupling (Figure 1C) where unidirectional connections from the population generating one rhythm actively modulate the other rhythm. So far, theoretical models of unidirectional coupling only considered the case where FO are driven by SO, although the reverse mechanism of FO driving SO might also exist [15]. Finally, unidirectional CFC with external drive (Figure 1D) corresponds to the case where SO is not an internally generated oscillation but is a (pseudo-)rhythmic sensory signal modulating FO in sensory circuits (see section 'Temporal Parsing of Continuous Stimuli').

In addition to the specific neural architectures, circuit parameters such as cross-circuit coupling strength also determine the temporal pattern of the cross-coupled oscillations. An important factor that characterizes the dynamics of CFC is whether the FO is present or not throughout the slow cycle [16]. Accordingly, we distinguish between continuous CFC, where the fast oscillations remain constantly active (Figure 1E), and intermittent CFC where FO is only present in a restricted interval of the SO cycle (Figure 1F,G). Both can be predicted from the phase diagram, which shows the conditions for fast oscillations to occur as a function of external inputs (Figure 1E–G) [13,17–19]. In the phase diagram, each phase of the SO cycle is associated with a given subset of coordinates, and the whole SO cycle determines a periodic trajectory. If the external modulation by the SO is weak enough that the FO state stays within the oscillatory region throughout the SO cycle (e.g., for weak coupling, Box 1), FO remains continuously active throughout the SO cycle. If, conversely, the SO is strong enough to drive the FO system in and out of the oscillatory region of the phase diagram (FO passes a bifurcation point at the boundary between the oscillatory and non-oscillatory region), FO occurs intermittently for SO phases where the FO system stays within the oscillatory boundaries. Within this scheme, FO can alternate with quiescent periods during which there is no spiking activity in the network (Figure 1F), with an asynchronous regime where spiking is not synchronized across neurons (Figure 1G), or any other dynamic state. Existing computational models of intermittent CFC have only focused on alternation with quiescent state [16,20].

[3]Department of Neuroscience, University of Geneva, Campus Biotech, 9 chemin des Mines, 1211 Geneva, Switzerland
[4]Group for Neural Theory, Institut National de la Santé et de la Recherche Médicale (INSERM) Unité 960, Département d'Etudes Cognitives, Ecole Normale Supérieure, 29 rue d'Ulm, 75005 Paris, France
[5]Centre for Cognition and Decision Making, National Research University Higher School of Economics, Myasnitskaya Street 20, Moscow 101000, Russia

*Correspondence: alexandre.hyafil@gmail.com (A. Hyafil).

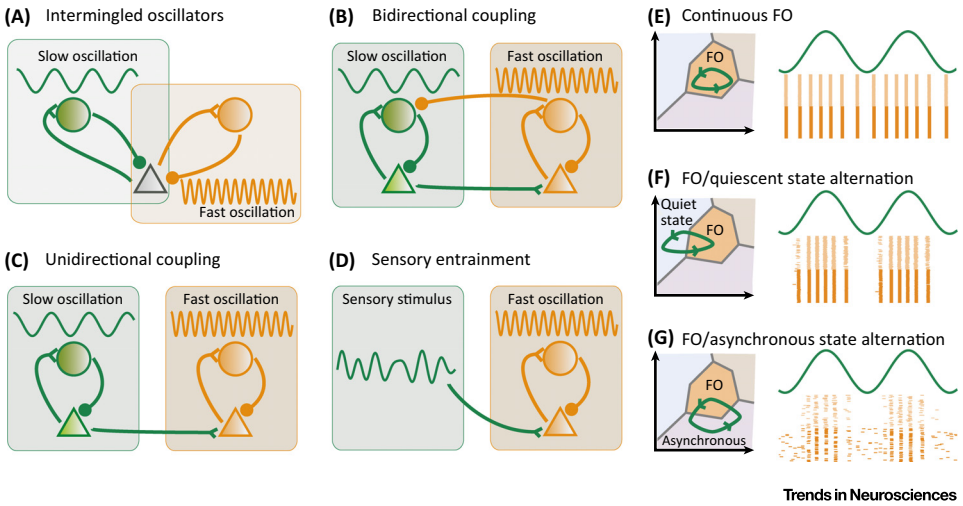

Figure 1. Architectures for Cross-Frequency Neural Coupling. (A–D) Cross-frequency coupling (CFC) architectures. (A) Intertwined oscillators. Neural oscillations in distinct frequency bands are generated by partially overlapping neural populations. In the depicted example, excitatory neurons (represented by the triangle) participates in the generation of both a slow oscillation (SO) and a fast oscillation (FO), whereas separate inhibitory populations (represented by green and orange circles) are involved in the generation of respectively SO and FO. CFC arises though the dynamics of the neural population common to both oscillations. Intermingled CFC has been proposed to explain the emergence theta/gamma coupled oscillations in hippocampus [6,30,100], where a common excitatory population is coupled to fast-spiking (FS) cells (generating gamma oscillations) and oriens-lacunosum moleculare (O-LM) cells (generating theta oscillations). (B) Bidirectional coupling. Segregated populations are implicated in the generation of the SO and FO (in the depicted example, a population of excitatory and inhibitory neurons for both oscillations), and coupling is mediated by reciprocal coupling between SO neurons and FO neurons. This architecture was used in the first computational model of coupled theta–gamma oscillations in hippocampus, which featured two coupled inhibitory subpopulations with distinct GABA decay time [101]. Moreover, precise spiking and local field potential (LFP) dynamics of *in vitro* cortical slices was explained by a sophisticated model whereby a beta1 rhythm concatenates two bidirectionally coupled oscillations, a gamma rhythm generated in superficial layers and a beta2 rhythm generated in deep layers [102,103]. (C) Unidirectional coupling. Distinct populations are implicated in the generation of SO and FO, and coupling arises though one population projecting onto the other population (here SO to FO). In a recent model of speech perception in auditory cortex, coupled theta–gamma oscillations were modeled by two separate excitatory–inhibitory subpopulations responsible for the generation of both rhythms [39], with the theta module projecting onto the gamma module. (D) Sensory entrainment. Sensory entrainment of neural oscillators is a special case of unidirectional coupling where a neural oscillator is modulated by slow modulations in sensory stimulus (e.g., visual rhythmic movements or amplitude-modulated sounds). This model has been tested in the context of visual processing: a PING module generating broad gamma rhythm responds to visual activity experimentally recorded in monkey thalamus that carries strong slow modulations [28]. (E–G) Temporal dynamics of FO. (E) Continuous FO. (Left) Schematic phase diagram of FO dynamical state: continuous FO occurs when SO modulation shapes a trajectory within the region of existence of FO. (Right) The continuous model of CFC from Fontolan *et al.* [16] (see their Figure 5) was transformed into a mathematically equivalent model of quadratic-and-fire neurons and simulated (with membrane white noise of variance 0.01). SO is modeled as a simple modulatory signal while FO is composed of a population of pyramidal and inhibitory cells generating gamma oscillations through the PING mechanism. (Top right) SO modulating signal. (Bottom right) raster plot of FO spikes: pyramidal neurons ($n = 50$, light orange); inhibitory neurons ($n = 50$, dark orange). FO spiking occurs throughout the SO cycle. (F) Oscillation/quiescent-state intermittent FO. (Left) This type of intermittent FO occurs when SO modulation shapes a trajectory between the oscillatory and quiescent regions of FO. (Right) The intermittent model of CFC from [16] (see their Figure 7) was transformed into network of quadratic-and-fire neurons and simulated. FO alternates between a period of gamma oscillations when excitation from SO is large enough, and a quiescent state when SO signal is lower. (G) Oscillation/asynchronous-state intermittent FO. (Left) This type of intermittent FO occurs when SO modulation shapes a trajectory between the oscillatory and asynchronous regimes of FO. (Right) We modified the parameters of the gamma network of [16] (constant current, synaptic conductance, and membrane noise) such that the network alternates within SO cycle between a period of strong oscillation and a period of asynchronous spiking activity.

Glossary

Amplitude–amplitude coupling (AAC): coupling between the amplitudes of a slow oscillation (SO) and a fast oscillation (FO).

Cross-frequency coupling (CFC): dynamical interactions between neural oscillations operating in different frequency bands.

Dense-spiking oscillation: oscillation generated by synchrony in a neural population in which each neuron in the population emits one spike per cycle at a specific phase.

Interneuronal gamma (ING) oscillation: gamma neural oscillation (>30 Hz) arising from inhibitory–inhibitory coupling; an inhibitory burst silences the network until synaptic inhibition decays.

***m:n* coupling:** form of phase–phase coupling where the FO completes exactly *m* cycles while the SO completes *n* cycles (e.g., 2:1, 3:1, or 3:2).

Phase–amplitude coupling (PAC): coupling between the phase of a SO and the amplitude and a FO, also known as 'nesting'.

Phase–frequency coupling (PFC): coupling between the phase of a SO and the frequency of a FO.

Phase–phase coupling (PPC): coupling between SO and FO phases.

Pyramidal interneuronal gamma (PING) oscillation: gamma neural oscillations (>30 Hz) arising from excitatory–inhibitory coupling; a burst of excitatory neuron spiking is closely followed by a burst of inhibitory spikes silencing the network until the next excitatory burst.

Sparse-spiking oscillation: oscillation generated by synchrony in a neural population in which spiking of individual neurons is stochastic; the oscillation frequency exceeds the average firing rate.

CFC Signatures

Experimentally, evidence for CFC derives from spectral analyses of collective neural measures [local field potential (LFP), electroencephalography (EEG), or magnetoencephalography (MEG) signals]. Each oscillation is characterized by three properties: frequency, amplitude, and phase. Theoretically, two rhythms may couple through any pair of such features, but coupling emerges

more readily when both features evolve on similar timescales. Hence, the four principal CFC signatures are: **phase–frequency coupling** (PFC), **phase–phase coupling** (PPC), **phase–amplitude coupling** (PAC), and **amplitude–amplitude coupling** (AAC) [4]. Recently, the development of novel statistical methods has allowed discrimination between the different coupling modes in recorded data [21–25].

Essentially, the challenge that experimentalists are facing is to infer the underlying network structure from CFC neural signatures measured from brain recordings [1,26]. Computational modeling of CFC networks provides clues as to how to resolve this non-trivial reverse-engineering problem (Box 2). A pivotal issue is the complex relationship between spiking activity, the focus of most network modeling studies, and the measures of collective neural activity, such as the LFP or EEG signal, on which most empirical evidence of CFC is based [27]. Because the frequency of an LFP oscillation reflects the frequency of average spiking of local populations, the observed oscillation is more visible in multi-unit rather than in individual spiking activity [28]. Moreover, power in an LFP oscillation reflects the degree to which neural spiking engages in a global oscillation, and is thus sensitive both to the fraction of neurons that spike at each cycle and to the phase dispersion of such spiking (i.e., the degree of synchronization). Finally, because LFP is assumed to index synaptic activity, there is usually a constant offset between the phase of the LFP oscillations and spike timing. Interestingly, such observed relationships should allow us to predict specific LFP signatures of distinct CFC networks.

Phase–Phase Coupling (PPC)

Much of our understanding on how and when two oscillations couple in phase arises from analyzing how the dynamics of coupled intrinsic oscillators can evolve towards a stable phase-locked solution (Box 1). PPC is a peculiar form of CFC that occurs even with very weak coupling. It is a subtle effect because both coupled variables (SO phase and FO phase) evolve along distinct timescales, and any perturbation due to heterogeneity or noise is liable to disrupt the coupling. The larger the *m* and *n* factors in ***m:n* coupling** (Box 1), the smaller the region of coupling parameter space where locking can occur [29].

Box 1. Analytical Methods for Neural Cross-Frequency Coupling

Dynamical systems theory provides powerful tools to study the different forms of coupling between cortical rhythms, using reduced mathematical descriptions of universal oscillatory phenomena to describe complex neural systems with relatively simple sets of differential equations. Different coupling classes can be organized according to the magnitude of the synaptic conductance present in the network. SO and FO are weakly coupled when the connections are weaker than the intrinsic forces driving each oscillator. In this case, amplitude modulations of FO are negligible, and one can fully describe the dynamics by the phase of the oscillations, giving rise to PPC. By contrast, strongly coupled systems may also lead to PFC, PAC, and AAC.

When synaptic SO–FO interactions are fast enough (the case referred to as 'pulsatile coupling'), one can compute the phase response curve (PRC) [104], that is, the phase advance/delay induced by a small synaptic perturbation as a function of the current phase of the oscillator (Figure IA–D). From the PRC one can then determine the FO-to-SO synchronization properties [105]: a fully nonnegative (type I) PRC produces a weak PPC but reliable PFC (Figure 2A); instead, a FO with biphasic (i.e., partly positive and partly negative, type II) PRC is prone to synchronize in phase with any SO, but yields more modest PFC. PRC shapes can be measured experimentally [106,107], and help to determine the FO-system bifurcation, in other words the particular set of key changes in its dynamics. The PRC formalism can be applied to both unsynchronized and phase-locked dynamics (*m:n* coupling). Regions of the parameter space correspond to different *m:n* locking modes, forming the Arnold tongue map of the system (Figure IE). Although the PRC is usually computed between two oscillators (neurons or populations), including bidirectional intermittent strongly coupled oscillations [108], it has been used to model complex multiple interactions such as three-neuron networks [20,109]. Similar methods are used for weakly coupled oscillations with slow synaptic coupling [110].

In stochastic networks with weak coupling, perturbation analysis can be applied to mean field models (e.g., the model of Wilson and Cowan [111]) to compute a first approximation of frequency modulations, in the case of PFC [18]. Novel perturbation methods to investigate continuous strong coupling are being developed [16,112], although a general theory is still lacking. In contrast to PPC and PFC, PAC is usually analyzed by reducing the population activity to a set of Wilson–Cowan equations [19,96]; however, the suitability of this simplification has not yet been thoroughly assessed.

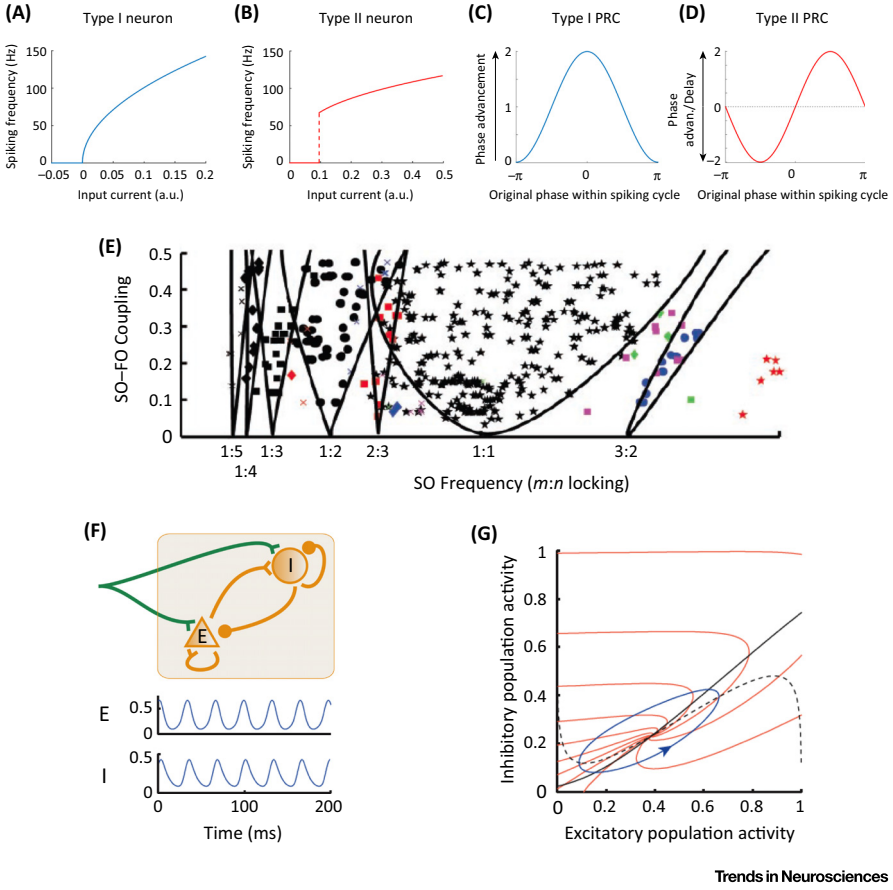

Figure I. (A,B) Spiking frequency of type I and type II neurons as a function of driving-current magnitude. (A) Cells with type I membrane excitability can spike at any arbitrary frequency once passed beyond the bifurcation point. (B) When a type II neuron goes through the bifurcation point it starts firing from a finite frequency. (C) Phase response curve of a type I neuronal oscillator: any small excitatory input induces a phase advance within the spiking cycle of the oscillator. (D) Phase response curve of a type II neuron: an excitatory pulse either advances or delays the next spike depending on the particular phase at which the input arrives within the spiking cycle. (E) When solicited with an external sinusoidal input (SO), individual neurons from *Aplysia* display Arnold tongue maps (i.e., different forms of *m:n* coupling depending on the input frequency and amplitude). Experimental results are in fair agreement with model simulations (adapted from [29]). (F,G) Phase–amplitude coupling modeled through a set of Wilson–Cowan equations to represent the activity of a specific population of interneurons in rat hippocampus (adapted from [96]). Experimenters recorded the response of excitatory and inhibitory neurons to sinusoidal inputs induced using optogenetics tools. (F) Schematic illustration of the excitatory–inhibitory hippocampal network and spontaneous FO visible in E and I population activity in absence of external noise. (G) Phase portrait of the FO model showing the stable limit cycle of the system (blue), the nullclines (i.e., the points where either the excitatory or the inhibitory activity would be constant; black: dashed, excitatory; solid, inhibitory), and the isochrones (the set of initial points from which the dynamics would evolve towards oscillations having the same phase; red). Phase and amplitude modulations of FO can be inferred from the phase portrait, given a specific set of initial conditions.

A recent analytical study shows how a **pyramidal interneuronal gamma** (PING) rhythm locks to a slow sinusoidal input both in the cases of continuous and intermittent FO/quiescent state regimes [16]. Whereas PPC is always weak in the continuous case (Figure 2A), strong FO synchronization occurs in the intermittent regime at every SO cycle, whenever the system crosses the bifurcation point to the quiescent state (Figure 2B). A similar strong phase-locking of gamma FO to theta SO is found in intermingled models of rat hippocampus coupled oscillations [6,20,30,31]. In this case, *m:n* synchronization is granted by an inhibitory pulse that shuts down

Box 2. Inferring CFC Architecture from Neural Data

Intermingled versus Independent Coupling

In intermingled models, resection of neural connections preserves one of the two rhythms. For example, transverse hippocampal slices display gamma activity only, while longitudinal slices show theta activity. Resection along one or the other direction severs the pyramidal–FS or pyramidal–O-LM connections, disrupting either of the two rhythms [100], consistent with an intermingled network where the pyramidal population is involved in the generation of both oscillations. By contrast, in an independent CFC network, two independent rhythms are preserved when the two subpopulations are resected, as is the case of the coupled gamma and beta2 rhythms generated respectively in deep and superficial layers of the neocortex [102]. In non-interventional experiments, CFC between distal sites (across areas or cortical layers) is strong indication for independent coupling, especially if it is stronger than local CFC [51].

Unidirectional versus Bidirectional Coupling

Within a SO cycle, the phases at which distinct neural subpopulations sequentially fire reflect the underlying causal chain of spiking, which can hence be retrieved using methods based on causal models of neural spiking [113–115]. The pharmacological blockade of firing activity can uncover the causal patterns of spikes, as was used in [103] to reveal a mechanism for rhythm concatenation in *in vitro* cortical slices. Causality is more difficult to evaluate when collective signals such as LFP or EEG, rather than spiking activity, are recorded. A recent analysis of CFC in intracortical signals during speech perception combined a non-causal measure of CFC and a causal measure of within-frequency coupling, revealing causal relationships between two distinct frequency bands in two distinct areas [116]. More recently, Jiang and colleagues developed an original technique to measure causality between distinct frequency bands and showed that, surprisingly, the power of gamma oscillations drives slower alpha oscillations in resting state [15] (Table I).

Table I. Summary of Systematic Relationships Between Network Architectures and CFC Signatures[a]

	FO PRC: Type I	FO PRC: Type II
Weak coupling	–	PPC
Strong coupling, continuous FO	Weak PPC, strong PFC	Strong PPC, weak PFC
	If sparse-spiking FO: PAC If sparse-spiking FO and asymmetric SO: AAC	
Strong coupling, intermittent FO/quiescent	PPC, PFC, PAC If asymmetric SO: AAC	
Strong coupling, intermittent FO/asynchronous	Weak PPC, PFC, PAC If asymmetric SO: AAC	

[a]See section (ii) in the main text and Box 1 for details.

network activity for a short period at every SO cycle; this requires SO inhibition to last longer than the membrane potential time-constant of the FO neuron. However, intermittent FO does not guarantee strong PPC: for example PPC is absent when the FO switches intermittently to the asynchronous regime (Figure 2C).

Phase–Frequency Coupling (PFC)

PFC is a generic form of CFC models where SO modulates the excitability of FO, which in turn induces a FO frequency modulation. In a continuous CFC setting, this modulation is bounded by a minimal and a maximal FO frequency generally corresponding to the trough and peak of the SO (Figure 2A). In intermittent CFC, the FO frequency is modulated during the periods of oscillatory regime, while outside this period FO is non-existent (Figure 2B,C). Such frequency modulation was analyzed in a noise-free dense-spiking PING FO network, under both continuous and intermittent CFC settings [16]. Simulations of a SO-modulated minimal PING model also showed that FO accelerates when the SO input whether to pyramidal cells or, counter-intuitively, to inhibitory cells [19], is maximal. Despite being a prevalent signature of CFC, PFC is seldom reported in experiments, presumably because it is difficult to identify instantaneous frequency peaks in EEG and MEG spectrograms. Nevertheless, PFC could be investigated in intracranial recordings, where clear peaks do appear even at higher frequencies [32,33]. Interestingly, PFC and PPC tend not to appear conjointly (Boxes 1,2). For example, the former appears without the

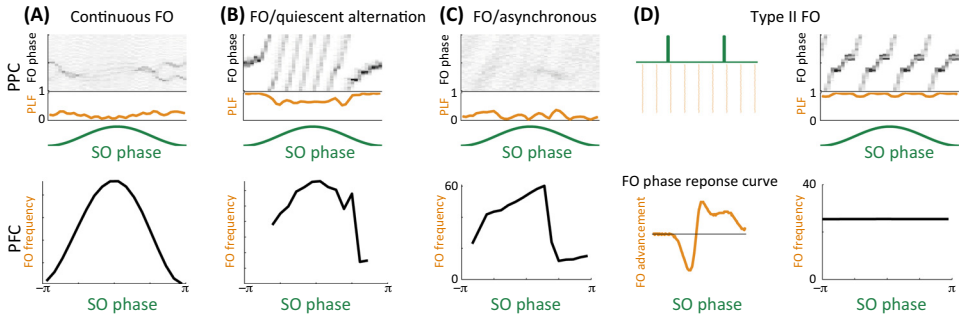

Figure 2. Phase–Frequency Coupling (PFC) and Phase–Phase Coupling (PPC). (A) Continuous fast oscillation (FO). (Top) PPC in the continuous FO model of Figure 1E. The top panel shows the histogram of FO phases as a function of slow oscillation (SO) phase for a simulation of 30 s. Darker areas show higher phase concentration. The overall largely homogeneous pattern indicates that very limited PPC emerges, which is confirmed by computing the FO phase-locking factor (PLF) as a function of SO phase [69]: low PLF indicates that SO phase had virtually no influence on FO phase. The green line shows the outline of the SO modulating signal. (Bottom) PFC in the same model. The black curve shows the frequency of FO bursts as a function of SO phase. (B) Intermittent oscillatory/quiescent FO. (Top) PPC in the intermittent oscillatory/quiescent FO model of Figure 1F. The top panel shows very strong FO phase concentration throughout the SO cycle, with nearly non-existent phase change during the quiescent period (i.e., frequency vanishes) and rapid phase dynamics in the oscillatory period. FO-PLF remains high during the whole SO cycle, with highest values during the quiescent period. (Bottom) PFC in the same model. FO frequency is modulated during the oscillatory period and vanishes during the quiescent period. (C) Intermittent oscillatory/asynchronous FO displaying PFC without PPC. (Top) PPC in the intermittent oscillatory/asynchronous FO model of Figure 1G. PPC hardly emerges in this network because no phase-resetting occurs during the asynchronous phase. (Bottom) PFC in the same model. FO frequency is modulated during the oscillatory period and vanishes during the asynchronous period. (D) Type II FO displaying PPC without PFC. (Top left) Raster plot of a network of a single class of interconnected excitatory neurons (adaptive quadratic integrate-and-fire) receiving rhythmic SO impulse. (Bottom left) Nearly symmetrical phase response curve (PRC) of FO neurons showing phase lead for later phases and phase lag for earlier phase, corresponding to a type II oscillator (Box 1). (Top right) Strong PPC in the network because type II oscillators phase-lock easily to external excitatory input. (Lower right) PFC is absent in the same network. Because of the symmetrical PRC, on average there is no acceleration or slowing down of the FO because phase leads and delays cancel out, and FO remains at a constant frequency throughout the SO cycle.

latter in intermittent FO/asynchronous networks (Figure 2C) while the opposite pattern is illustrated in Figure 2D. These two examples show how different coupling architectures may give rise to fully distinct CFC profiles.

Phase-Amplitude Coupling (PAC)

PAC or nesting refers to the CFC case where FO power is modulated by the SO phase. PAC has been reported at many distinct frequency ranges and using various recording and computation techniques [5,34,35]. In intermittent CFC, PAC results from the presence of FO in only part of the SO cycle, such that FO power shows all-or-none switches [19,31]. PAC in continuous CFC is subtler and requires that SO modulates either the proportion or the phase dispersion of FO neuron spiking. Spiking patterns of individual neurons within the FO can span a whole spectrum from one spike per cycle to random, extremely sparse, spiking skipping multiple periods [13]. It is instructive to consider the two limiting cases as a conceptual scaffold to understand the mechanisms of CFC and their implications for function. In **dense-spiking oscillations** each neuron spikes once per cycle at a specific phase, leaving no opportunity for the slow rhythm to modulate either the proportion or the phase dispersion of spiking. As a consequence, PAC is absent when a dense-spiking PING FO is modulated by SO (Figure 3A), as well as in a simplified noise-free PING network [19]. By contrast, in the sparse-spiking PING case, when neuronal spiking is irregular and occurs at a much lower rate that the oscillation frequency [36,37], the number of neurons firing at each cycle and their phase-locking to the FO oscillations depends on the input parameters. As a result, a SO modulation yields strong amplitude modulation, in other

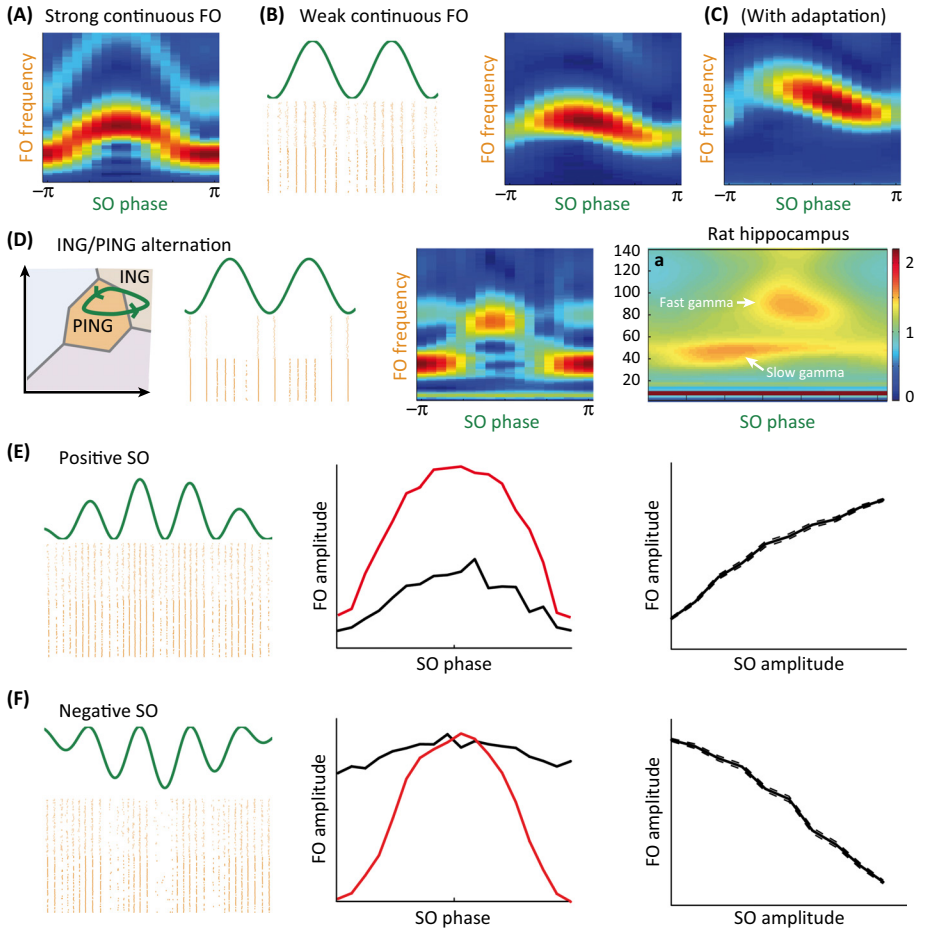

Trends in Neurosciences

Figure 3. Phase–Amplitude Coupling (PAC) and Amplitude–Amplitude Coupling (AAC). (A) Dense-spiking continuous fast oscillation (FO). Plot shows FO amplitude as a function of slow oscillation (SO) phase for distinct FO frequencies (from 10 Hz to 100 Hz) for the dense-spiking continuous FO model of Figure 1E. Red, high FO power; blue, low FO power. Peak FO frequency varies throughout SO cycle (PFC) but the overall FO power remains constant. (B) Sparse-spiking continuous FO. PAC is present in a model identical to that of panel A with simply an increased level of noise, producing sparse-spiking FO oscillations. (Left) Raster plot showing that the number of FO spikes at each cycle varies as a function of SO phase. (Right) FO amplitude as a function of SO phase, showing strong PAC with maximal FO amplitude close to SO peak, on top of PFC. (C) Sparse-spiking continuous FO with adaptation. The model in (B) was modified by introducing an adaptation current, slowing down the dynamics of the FO oscillation in response to SO modulation. PAC plot shows that maximal FO power occurs at a later SO cycle compared with the no-adaptation model of (B). (D) Dual ING/PING alternation. (Leftmost and middle-left) The FO network alternates within a SO cycle between a period of pyramidal-interneuron-generated oscillations (PING mechanism) and another period of faster interneuron-generated oscillations (ING) (this is obtained by a SO modulation applied to the inhibitory instead of the excitatory population). (Middle-right) FO amplitude as a function of SO phase. PAC occurs for two distinct FO frequencies, with maximal FO power for these two frequencies in antiphase. Such a pattern with distinct frequencies (pointing to distinct oscillation-generation mechanisms) should not be confounded with the case of a frequency modulation within a single FO frequency band, as shown in (A). (Rightmost) Data from rat hippocampus recordings showing a similar alternation between slow gamma and fast gamma within a theta cycle (adapted from [41]). (D) Positive AAC for positive asymmetric SO. (Left panel) The cross-frequency coupling (CFC) network with sparse-spiking FO oscillations was simulated with a SO sinusoid which amplitude was modulated at a 1 Hz rate, whereby an increase in SO amplitude is accompanied by a general increase in SO level (green curve, left panel). This leads to general increase of FO amplitude on top of an increase of PAC strength. (Middle panel) FO amplitude as a function of SO phase, separately for high SO amplitude cycles (red curve) and low SO amplitude cycles (black curve). PAC was present as for the non-modulated SO sinusoid (Figure 3B), but here PAC modulation increased with higher SO amplitude. (Right panel) FO amplitude as a function of SO amplitude, showing strong positive AAC. Figure S1 in the supplemental information online shows the absence of AAC for a symmetric SO. (F) Negative AAC for negative asymmetric SO. Same model as in (E) but here the increase in SO amplitude is accompanied by a general decrease in SO level. This in turn leads to general decrease of FO amplitude on top of an increase of PAC strength, hence a negative correlation between SO and FO amplitudes.

words PAC (Figure 3B) [38,39]. **Sparse-spiking** gamma **oscillations** are prominent in sensory areas and respond to the sensory input. Accordingly, gamma power which reflects the information content of the stimulus is modulated by slow (delta) fluctuations of the sensory stimulus [28,40].

The precise dependence of FO power on SO phase reflects the underlying coupling mechanisms [19]. In general, one expects FO power to be maximal at SO peak or trough, depending on the excitatory/inhibitory nature of SO. Accordingly, electrocorticography (EcoG) recordings in human patients reveal that inter-areal PAC occurs mainly when FO power is maximal around SO peak or trough [35]. However, transmission and synaptic delays as well as neural adaptation may introduce a significant phase-shift (Figure 3C). This likely explains why, for some electrode pairs, FO power peaks with some offset with respect to SO extrema [35].

An interesting configuration emerges when SO modulation induces a switch in FO between two distinct oscillatory modes, for example, between a slower PING-like oscillation and a faster **interneuronal gamma** (ING) (Figure 3D). In this case, the power of both FO oscillations couples in antiphase to the SO. Accordingly, low and high gamma power peaking at distinct phases of a theta cycle has been observed in both the hippocampus and the motor cortex [41,42]. The alternating PING/ING scenario mentioned above appears to be a possible oscillation generation mechanism in these circuits.

Amplitude–Amplitude Coupling (AAC)

While there is an abundant literature on amplitude coupling of neural oscillations in the same frequency band at distal sites [43–46], within- and cross-frequency AAC probably rely on distinct neural mechanisms. Within-frequency AAC is simply a marker of linear coupling, and is thus not very specific with respect to the underlying mechanisms. By contrast, cross-frequency AAC emerges when SO power modulates the average FO power; this occurs on top of PAC when the SO shape is asymmetric. For positive asymmetric SO, that is, when the overall SO level increases with power and SO positively modulates FO amplitude, higher SO amplitudes lead to overall higher FO amplitudes, and there is positive AAC (Figure 3E). This was observed in a model of sparse-spiking sensory gamma modulated by theta sensory signals (see Figure 4F in [40]). AAC can also emerge from a negative asymmetric SO, leading to a negative correlation between SO and FO amplitudes (Figure 3F). The human visual alpha oscillation is asymmetric [47] and is thought to be functionally inhibitory [48,49]. Accordingly, alpha increases are typically accompanied by gamma decreases in occipital areas [10,50,51]. Moreover, the alpha phase modulates gamma amplitude (AAC is accompanied by PAC) and stronger alpha power increases PAC [52,53].

Functions of CFC

The ubiquity of CFC phenomena across dynamical systems, from seismic waves to financial indices [54], challenges the relevance of these phenomena to brain function. As illustrated above, in most cases at least one form of CFC signatures is bound to emerge from intrinsically shared circuitry, or from connections between neural systems generating oscillations at distinct frequencies. Given this uncertainty, the issue of how coupled neural oscillations contribute to cognitive operations has been the object of intense exploration and speculation. Reviewing the possible CFC mechanisms and their related dynamical signatures significantly enhances the possibility to connect CFC as empirical phenomena to specific neural computations, and permits a reasonable bridge to brain functions, which are grouped below into three conceptual families.

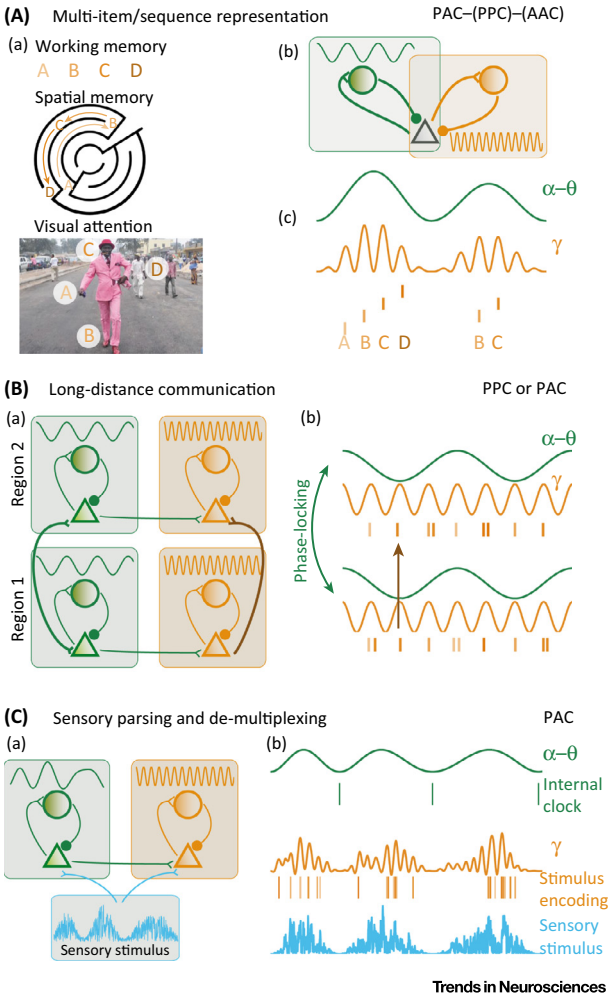

Figure 4. Functions of Cross-Frequency Coupling (CFC). (A) Multi-item/sequence representation. (a) Multi-item representations through CFC is envisaged for working memory (Top, in hippocampus and prefrontal cortex) [54,116], spatial memory for previously and subsequently visited items (in hippocampus) [60,61], and visual attention to a series of items in visual field (Bottom, in visual cortex) [10]. (b) Putative CFC architecture for multi-item representation. Intertwined CFC network with a common population of pyramidal neurons connecting to two populations of distinct types of inhibitory neurons, each responsible for the generation of one of the two oscillations (slow, SO; and fast, FO). Some models also include direct connections between the two inhibitory populations [6,20]. (c) Multi-item representation relies on intermittent/quiescent CFC regime: the nested FO oscillation only occurs during a defined phase range, with one item being represented at each FO burst. AAC (through asymmetrical SO) allows modulating the phase range of FO and thus the number of represented items. (B) Long-distance communication. (a) Putative architecture. FO synchrony between region 1 and region 2 is mediated by inter-area SO synchrony and local PPC. Strong SO coherence is provided by connections between the two SO modules (broad green connection). As a result, FO synchrony allows efficient selective communication between region 1 and region 2 neurons (broad orange connection) in face of distractors. (b) Coherent SO oscillations (green lines), coherent FO oscillation (orange lines). The rastergram below the oscillatory pattern in each region shows that the spiking pattern in region 2 closely follows that of region 1. (C) Sensory parsing. (a) Putative architecture: a sensory stimulus (light blue) with slow rhythmic modulations is fed both to a SO module whose activity phase-locks to sensory modulations (green), and to a FO module that encodes fine-grained stimulus information (orange). Direct connection from SO to FO enables control of stimulus-processing resources depending on the modulation phase, with more FO power being assigned to more-informative stimulus periods [39]. (b) Sensory decoding: SO provides an internal clock for stimulus decoding; for example, FO spikes can be decoded with respect to SO spike bursts. FO is nested within FO, and the stimulus is encoded in pattern of spikes from the FO module.

Multi-Item or Sequence Encoding

Many neural systems need to concurrently maintain active representations of distinct items, while avoiding interferences: these can be objects in the visual field, items in working memory, or sequences of motor commands in a complex movement [4]. Neural oscillations offer a potentially efficient tool for multi-item representation by temporally clustering spikes pertaining to each item within distinct oscillations phases. This principle allows downstream neural systems to read-out a given item by tuning to its associated phase range [55,56]. CFC offers a refined version of this phase-clustering scheme: the SO oscillation defines the phase-coding temporal code while the FO oscillation generates rhythmic spiking activity, associating each represented item with one FO cycle (Figure 4A). The discrete item-specific FO bursts within the SO cycle optimize the encoded information while minimizing interference across encoded items. This idea dates back to a model proposed by Lisman and colleagues, wherein items representations were nested within coupled hippocampal theta–gamma rhythms [57,58]. Similarly, alpha–gamma CFC over parietal–occipital networks is proposed to underpin multiple-item representation in visual working memory [59]. CFC also provides a means of ordering a timed sequence of elements within a time-compressed temporal window, which appears potentially useful to learn specific associations between the successive elements (through neural plasticity) [12]. This coding principle is hypothesized to underpin spatial navigation in the rodent hippocampus: within a theta cycle a full sequence of locations, from previously to subsequently visited locations, is represented at a rate of one location per gamma cycle [60,61]. Likewise, alpha–gamma CFC assemblies are proposed to mediate cortical representation of sequences of visual field locations [10,62]. The activation order of neural representations within an alpha cycle would depend on stimulus saliency: neurons coding for the most salient stimuli activate first and process information in priority, while less-salient stimuli are processed later, and irrelevant stimuli may even not be processed at all.

What neural architecture(s) and CFC signature(s) could possibly support multi-item representation? CFC-based multi-item representation is characterized by one inactive period within the SO cycle (specifically, between the beginning of a new sequence and the end of the previous one) during which no item is represented and FO vanishes. It thus corresponds to an intermittent FO CFC, potentially inducing both PAC and PPC. Hippocampal theta–gamma PAC has been reported across studies in rodents [30,63] and humans [64,65]. PAC increases during learning of item–context associations [66] and *m:n* PPC between theta and low- and mid-gamma frequencies is present during maze exploration, on top of a PAC effect [67]. Theta–gamma PPC is observed in human EEG during visual working memory [68], with a load-dependent PPC effect during retention of visual information in addition to PAC [69]. Circuit models of coupled theta–gamma generation reproduce such dynamics, using intermingled theta–gamma network modules producing intermittent gamma/quiescent CFC, and thus PAC and PPC [6,30]. In the framework of these models, the maximum number of items that can be simultaneously represented is determined by the number of active FO cycles within one SO. The models account for the proposed maximal number of items (7 ± 2) that can be stored in human short-term memory because at most seven gamma cycles can fit within a theta cycle [57]. Interestingly, storage capacity could acutely be modulated by modifying the SO frequency, as observed during high-load working-memory tasks [9].

AAC provides an alternative mechanism: the amplitude of SO would modulate the number of FO cycles and thus the number of represented items. This scheme could account for the modulation of visual field capacity as a function of attention: when attention is low, the visual alpha band power increases in the related visual field, and, through its inhibitory action on spiking gamma activity (negative AAC), restricts the amount of attended items to the most salient ones [10]. In turn, top-down control of visual attention may implicate a whole hierarchy of oscillations. Occipital alpha is modulated by frontal theta through negative AAC: this would explain why

increases in frontal activity after behavioral errors are translated into decreases in occipital alpha, and thus enhanced attention [70]. Such a top-down regulation of visual processing through AAC is absent in children with attention deficit hyperactivity disorder (ADHD) performing a cross-modal task, and could account for their cognitive impairment on the task [71]. For spatial navigation, positive AAC is proposed to play a similar role: theta–gamma AAC increases during successful spatial navigation based on trial-and-error exploration [72].

Synchronization of Fast Oscillations for Long-Distance Communication

One of the most prominent roles assigned to neural oscillations is to mediate selective neural communication between areas, with in-phase regions communicating more efficiently than out-of-phase ones [73]. Gamma rhythms have predominantly been implicated in this so-called 'communication through coherence' mechanism, especially for bottom-up processes [74]. However, fast oscillations only synchronize at a local scale. By contrast, slower rhythms (<10 Hz) may synchronize between distant areas [75,76]. Coupling phase of gamma oscillations to slower rhythms may be a way to selectively enhance communication between distant areas via long-distance synchronization between local gamma rhythms [12,59]. In this way coherence between distant SO associated with local SO/FO PPC could bring synchrony to distant FO (Figure 4B). Accordingly, observations in rodents show fast gamma synchronization between hippocampus CA1 and medial entorhinal cortex, slow gamma synchronization between CA1 and CA3, theta synchrony between all three sites, and a strong coupling of low and high gamma to theta [41]. A computational model of hippocampal theta–gamma oscillations demonstrates mechanistically how theta synchronizes gamma in transverse CA3 modules [6]. A similar mechanism might be at work in visual cortex, where theta phase modulates V1/V4 gamma synchronization during a selective attentional task [77,78]. These observations are consistent with a form of PPC where gamma is reset by the theta oscillation. However, good FO synchronization requires precise SO alignment at the FO timescale. For example, in the hippocampus model, gamma synchronizes across modules when theta conduction delays are below 8–9 ms, in other words only a fraction of the ~40 Hz gamma cycle [6].

A variant of the communication through CFC hypothesis postulates increased communication between regions in which gamma is jointly active within similar SO phases; this scheme requires PAC rather than PPC. In this view, the diversity of FO amplitude to SO locking could flexibly shape functional connectivity in the brain [35]. Evidence for such a routing mechanism comes from the medial temporal cortex: oscillations occurring in distinct gamma sub-bands and distinct portions of the theta cycle could ensure selective communication between CA1 and CA3, or between CA1 and medial entorhinal cortex [41]. This role of CFC is supported by recent *in vitro* measurements in human neocortical slices where interlaminar theta coherence coexists with theta–gamma PAC, and these two measures correlate [79]. A functional validation of this hypothesis comes from a task manipulating visual spatial attention in monkeys while activity was recorded from two interconnected regions of the ventral stream, V4 and TEO. As the monkey was paying attention to a given visual stimulus, there was an increase both in theta coherence between V4 site and TEO sites whose receptive fields encompass the location of the stimulus, and in theta–gamma PAC within each site [80]. This combination of distinct effects could selectively enhance communication across sites whenever the stimulus within their receptive field is the current focus of attention.

Temporal Parsing of Continuous Stimuli

Many biological stimuli are characterized by an intrinsic quasi-rhythmic temporal structure, or are processed in a rhythmic mode. Speech is marked with syllabic contours, odors are sniffed at the respiratory rhythm, visual scenes are explored at the pace of saccades, etc. [81,82]. While slow oscillations in sensory areas reflect the rhythm of the sensory signal or of sensory sampling, fast

gamma oscillations underpin fine-grained sensory processing in a bottom-up fashion [28,39,74,83]. The gamma rhythm does not need to have any counterpart in the sensory structure but is rather the operating rhythm of the sensory cortex itself. Hence, in this case, the FO represents the content and SO the context.

The control of FO by SO exploits the sensory temporal modulation during perceptual processes in two possible ways (Figure 4C) [8,84–86]. First, when the rhythm is present in the sensory signal, the cortical perceptual system may take advantage of the temporal structure of the input to perform discrete processing of meaningful sequences [82]. Slow oscillations (2–12 Hz) constitute the perfect tool for carrying such temporal predictions associated with rhythmic modulations [87]. There is ample evidence that slow oscillations in sensory areas lock to sensory input modulations [88,89], and could constitute an internal clock for chunking sensory stimuli (e.g., into syllables) and decoding FO activity. Correspondingly, the phase at which neurons in the auditory cortex spike with respect to slow LFP oscillations helps to uncover the identity of naturalistic sounds [90,91]. In a recent modeling work, we showed that theta spike bursts in auditory cortex can reliably signal the boundaries between syllables in continuous speech, thus parsing speech into relevant stimulus chunks; the identity of syllables can be decoded from the spike timing of FO (gamma) neurons with respect to SO (theta) spike bursts [39].

Second, SO may directly modulate FO to deploy more processing resources (FO power) at the SO phases where the most relevant sensory information occurs (e.g., onset of odors in sniffing episodes) and filter out irrelevant stimuli arriving out of phase [5,92,93]. In our syllable decoding model, direct connection between circuits generating slow and fast oscillations, essentially coupling gamma power to theta phase, was crucial to accurate syllable decoding.

Current Limitations and Future Directions

The field of neural cross-frequency coupling is still in its infancy. On the mathematical side, there is still much to do to understand the conditions under which CFC emerges (see Outstanding Questions). While most current theoretical studies focus on the synchronizing properties of individual neurons, we also need to understand the dynamics of populations of oscillating neurons (FO and SO), especially in the context of noise and heterogeneity [18,19]. Most importantly, theoretical work should be translated into testable experimental predictions with respect to the neural signatures of CFC (PPC, PAC, etc.).

Correspondingly, experimental studies should strive to pinpoint more specifically which type of CFC is encountered by testing its diverse forms in a given dataset. Too often, experimenters seek evidence for only one specific form of CFC, but the conclusion that a coupling mode does exist is, by itself, insufficient to link it to a particular neural architecture or function. Convergence between models and experiments should, when possible, be tested quantitatively and not only qualitatively, for example, by using model-based analyses to compare different possible architectures and infer physiological variables from experimental data.

Regarding the functional significance of CFC, the current challenge is to go beyond correlative observations of CFC signatures and cognitive processes. Computational modeling provides a promising tool because it allows direct testing of whether a biologically plausible neural circuit may implement a given cognitive operation. The three possible roles of CFC outlined here (multi-item representation, long-distance communication, sensory parsing) rely on substantial experimental evidence but all await validation from modeling (Outstanding Questions). The syllable parsing and recognition model we recently developed provides a first step in this direction, indicating that a theta–gamma sensory parsing could indeed work for the special case of speech perception [39]. For multi-item representation, this may involve constructing models of coupled theta–gamma generation with models of theta spatial encoding in hippocampus [6,94,95]. In

general, the CFC schemes will have to prove their functional relevance in comparison to alternative non-oscillatory encoding models. In complement to computational modeling, optogenetics provides a causal tool to intervene on the mechanisms of generation of coupled oscillations and pin down the specific role of CFC and of distinct neural subpopulations [96].

Concluding Remarks

The coupling between neural oscillations may take a variety of forms, emerge from different architectures, and underpin distinct functions. However, causal relationships between neural CFC and cognitive functions are yet to be demonstrated. We hope that, by clarifying the concepts and the relationships between mechanisms and function, the framework we outlined here will stimulate original research and hence contribute to filling conceptual and empirical gaps. Essential future developments in this research agenda include combining theoretical and experimental work, in particular using optogenetics to test the dependence of various cognitive operations on specific forms of CFC.

Supplemental Information

Supplemental information associated with this article can be found online at doi:10.1016/j.tins.2015.09.001.

Outstanding Questions

Can recent optimal and efficient coding theories [97] help to delineate clear and specific functional roles for CFC? Beyond mere phenomenological approaches, computational modeling using realistic neural networks together with optimality constraints will be necessary to prove the utility of CFC-based mechanisms for neural processing.

Can the general rules linking network physiology to CFC signatures presented in this review (and summarized in Table I in Box 2) be explained in a mathematical theory of neural CFC? These rules were distilled by generalizing from various computational studies focusing on specific neural networks; their validity needs to be confirmed using the tools of dynamic systems analysis.

How can we distinguish CFC as a functional feature of cognitive processes from CFC as a dynamic epiphenomenon? This is a very challenging point. Direct intervention that selectively manipulates levels of CFC while leaving other network properties unchanged could prove causality but looks unrealistic in the near future.

Is a realistic neural network generating coupled theta–gamma oscillations able to underpin multi-item representations? Proof-of-concept of the general multi-item representation framework was presented in seminal work from late nineties [98] using an overly simplified neural network. Such work should be adapted to take into account the more recent advances in our understanding of the generation of coordinated hippocampal theta–gamma oscillations [6,30].

Does specific long-distance communication improve when local gamma oscillations are locked to global slow oscillations [99]? The two alternative mechanisms, depending on whether the phase or amplitude of gamma locks to slow oscillations (i.e., PPC vs PAC), should be compared and contrasted both in computational models and experiments.

Are alternative, non-CFC, models more efficient for multi-item encoding, communication through coherence, and sensory de-multiplexing? Ultimately, functional models of CFC should be compared with alternative models not

References

1. Wang, X. (2010) Neurophysiological and computational principles of cortical rhythms in Cognition. *Physiol. Rev.* 90, 1195–1268
2. Ray, S. and Maunsell, J.H.R. (2014) Do gamma oscillations play a role in cerebral cortex? *Trends Cogn. Sci.* 19, 78–85
3. Young, C.K. and Eggermont, J.J. (2009) Coupling of mesoscopic brain oscillations: recent advances in analytical and theoretical perspectives. *Prog. Neurobiol.* 89, 61–78
4. Jensen, O. and Colgin, L.L. (2007) Cross-frequency coupling between neuronal oscillations. *Trends Cogn. Sci.* 11, 267–269
5. Canolty, R.T. and Knight, R.T. (2010) The functional role of cross-frequency coupling. *Trends Cogn. Sci.* 14, 506–515
6. Tort, A.B.L. *et al.* (2007) On the formation of gamma-coherent cell assemblies by oriens lacunosum-moleculare interneurons in the hippocampus. *Proc. Natl. Acad. Sci. U.S.A.* 104, 13490–13495
7. Lisman, J.E. and Jensen, O. (2013) The theta–gamma neural code. *Neuron* 77, 1002–1016
8. Giraud, A-L. and Poeppel, D. (2012) Cortical oscillations and speech processing: emerging computational principles and operations. *Nat. Neurosci.* 15, 511–517
9. Axmacher, N. *et al.* (2010) Cross-frequency coupling supports multi-item working memory in the human hippocampus. *Proc. Natl. Acad. Sci. U.S.A.* 107, 3228–3233
10. Jensen, O. *et al.* (2014) Temporal coding organized by coupled alpha and gamma oscillations prioritize visual processing. *Trends Neurosci.* 37, 357–369
11. Jensen, O. *et al.* (2012) An oscillatory mechanism for prioritizing salient unattended stimuli. *Trends Cogn. Sci.* 16, 200–206
12. Fell, J. and Axmacher, N. (2011) The role of phase synchronization in memory processes. *Nat. Rev. Neurosci.* 12, 105–118
13. Börgers, C. and Kopell, N.J. (2005) Effects of noisy drive on rhythms in networks of excitatory and inhibitory neurons. *Neural Comput.* 17, 557–608
14. Vierling-Claassen, D. *et al.* (2010) Computational modeling of distinct neocortical oscillations driven by cell-type selective optogenetic drive: separable resonant circuits controlled by low-threshold spiking and fast-spiking interneurons. *Front. Hum. Neurosci.* 4, 198
15. Jiang, H. *et al.* (2015) Measuring directionality between neuronal oscillations of different frequencies. *Neuroimage* 118, 359–367
16. Fontolan, L. *et al.* (2013) Analytical insights on theta-gamma coupled neural oscillators. *J. Math. Neurosci.* 3, 16
17. Brunel, N. (2000) Dynamics of sparsely connected networks of excitatory and inhibitory spiking neurons. *J. Comput. Neurosci.* 8, 183–208
18. Ledoux, E. and Brunel, N. (2011) Dynamics of networks of excitatory and inhibitory neurons in response to time-dependent inputs. *Front. Comput. Neurosci.* 5, 25
19. Onslow, A.C.E. *et al.* (2014) A canonical circuit for generating phase–amplitude coupling. *PLoS ONE* 9, e102591
20. Malerba, P. and Kopell, N.J. (2012) Phase resetting reduces theta–gamma rhythmic interaction to a one-dimensional map. *J. Math. Biol.* 66, 1361–1366
21. Aru, J. *et al.* (2014) Untangling cross-frequency coupling in neuroscience. *Curr. Opin. Neurobiol.* 31C, 51–61
22. Canolty, R.T. *et al.* (2012) Multivariate phase–amplitude cross-frequency coupling in neurophysiological signals. *IEEE Trans. Biomed. Eng.* 59, 8–11
23. Özkurt, T.E. and Schnitzler, A. (2011) A critical note on the definition of phase–amplitude cross-frequency coupling. *J. Neurosci. Methods* 201, 438–443
24. Palva, J.M. *et al.* (2005) Phase synchrony among neuronal oscillations in the human cortex. *J. Neurosci.* 25, 3962–3972
25. Jirsa, V.K. and Müller, V. (2013) Cross-frequency coupling in real and virtual brain networks. *Front. Comput. Neurosci.* 7, 78
26. Fletcher, M.L. *et al.* (2005) High-frequency oscillations are not necessary for simple olfactory discriminations in young rats. *J. Neurosci.* 25, 792
27. Denker, M. *et al.* (2011) The local field potential reflects surplus spike synchrony. *Cereb. Cortex* 21, 2681–2695
28. Mazzoni, A. *et al.* (2008) Encoding of naturalistic stimuli by local field potential spectra in networks of excitatory and inhibitory neurons. *PLoS Comput. Biol.* 4, e1000239
29. Hunter, J.D. and Milton, J.G. (2003) Amplitude and frequency dependence of spike timing: implications for dynamic regulation. *J. Neurophysiol.* 90, 387–394
30. Wulff, P. *et al.* (2009) Hippocampal theta rhythm and its coupling with gamma oscillations require fast inhibition onto parvalbumin-positive interneurons. *Proc. Natl. Acad. Sci. U.S.A.* 106, 3561–3566
31. Kopell, N.J. *et al.* (2010) Gamma and theta rhythms in biophysical models of hippocampal circuits. In *Hippocampal Microcircuits* (Cutsuridis, V., ed.), pp. 423–457, Springer
32. Ray, S. and Maunsell, J.H.R. (2010) Differences in gamma frequencies across visual cortex restrict their possible use in computation. *Neuron* 67, 885–896
33. Roberts, M.J. *et al.* (2013) Robust gamma coherence between macaque V1 and V2 by dynamic frequency matching. *Neuron* 78, 523–536

34. Schroeder, C.E. and Lakatos, P. (2009) Low-frequency neuronal oscillations as instruments of sensory selection. *Trends Neurosci.* 32, 9–18
35. Van der Meij, R. *et al.* (2012) Phase–amplitude coupling in human electrocorticography is spatially distributed and phase diverse. *Brain Cogn.* 32, 111–123
36. Brunel, N. *et al.* (2001) Effects of synaptic noise and filtering on the frequency response of spiking neurons. *Phys. Rev. Lett.* 86, 2186–2189
37. Brunel, N. and Hakim, V. (1999) Fast global oscillations in networks of integrate-and-fire neurons with low firing rates. *Neural Comput.* 11, 1621–1671
38. Spaak, E. *et al.* (2012) Hippocampal theta modulation of neocortical spike times and gamma rhythm: a biophysical model study. *PLoS ONE* 7, e45688
39. Hyafil, A. *et al.* (2015) Speech encoding by coupled cortical theta and gamma oscillations. *Elife* 4, 1–23
40. Mazzoni, A. *et al.* (2010) Understanding the relationships between spike rate and delta/gamma frequency bands of LFPs and EEGs using a local cortical network model. *Neuroimage* 52, 956–972
41. Colgin, L.L. *et al.* (2009) Frequency of gamma oscillations routes flow of information in the hippocampus. *Nature* 462, 353–357
42. Igarashi, J. *et al.* (2013) A theta–gamma oscillation code for neuronal coordination during motor behavior. *J. Neurosci.* 33, 18515–18530
43. Siegel, M. *et al.* (2012) Spectral fingerprints of large-scale neuronal interactions. *Nat. Rev. Neurosci.* 13, 20–25
44. Hipp, J.F. *et al.* (2012) Large-scale cortical correlation structure of spontaneous oscillatory activity. *Nat. Neurosci.* 15, 884–890
45. Brookes, M.J. *et al.* (2011) Investigating the electrophysiological basis of resting state networks using magnetoencephalography. *Proc. Natl. Acad. Sci. U.S.A.* 108, 16783–16788
46. De Pasquale, F. *et al.* (2012) A cortical core for dynamic integration of functional networks in the resting human brain. *Neuron* 74, 753–764
47. Mazaheri, A. and Jensen, O. (2008) Asymmetric amplitude modulations of brain oscillations generate slow evoked responses. *J. Neurosci.* 28, 7781–7787
48. Klimesch, W. *et al.* (2007) EEG alpha oscillations: the inhibition-timing hypothesis. *Brain Res. Rev.* 53, 63–88
49. Haegens, S. *et al.* (2011) α-Oscillations in the monkey sensorimotor network influence discrimination performance by rhythmical inhibition of neuronal spiking. *Proc. Natl. Acad. Sci. U.S.A.* 108, 19377–19382
50. Jensen, O. and Mazaheri, A. (2010) Shaping functional architecture by oscillatory alpha activity: gating by inhibition. *Front. Hum. Neurosci.* 4, 186
51. Spaak, E. *et al.* (2012) Layer-specific entrainment of gamma-band neural activity by the alpha rhythm in monkey visual cortex. *Curr. Biol.* 22, 2313–2318
52. Osipova, D. *et al.* (2008) Gamma power is phase-locked to posterior alpha activity. *PLoS ONE* 3, e3990
53. Roux, F. *et al.* (2013) The phase of thalamic alpha activity modulates cortical gamma-band activity: evidence from resting-state MEG recordings. *J. Neurosci.* 33, 17827–17835
54. He, B.J. *et al.* (2010) the temporal structures and functional significance of scale-free brain activity. *Neuron* 66, 353–369
55. Jensen, O. (2001) Information transfer between rhythmically coupled networks: reading the hippocampal phase code. *Neural Comput.* 13, 2743–2761
56. Akam, T.E. and Kullmann, D.M. (2010) Oscillations and filtering networks support flexible routing of information. *Neuron* 67, 308–320
57. Lisman, J.E. and Idiart, M. (1995) Storage of 7 ± 2 short term memories in oscillatory subcycles. *Science* 267, 1512–1515
58. Jensen, O. and Lisman, J.E. (2005) Hippocampal sequence-encoding driven by a cortical multi-item working memory buffer. *Trends Neurosci.* 28, 67–72
59. Roux, F. and Uhlhaas, P.J. (2013) Working memory and neural oscillations: alpha-gamma versus theta–gamma codes for distinct WM information? *Trends Cogn. Sci.* 18, 16–24
60. Lisman, J.E. (2005) The theta/gamma discrete phase code occuring during the hippocampal phase precession may be a more general brain coding scheme. *Hippocampus* 15, 913–922
61. Lisman, J.E. and Buzsáki, G. (2008) A neural coding scheme formed by the combined function of gamma and theta oscillations. *Schizophr. Bull.* 34, 974–980
62. VanRullen, R. (2003) Is perception discrete or continuous? *Trends Cogn. Sci.* 7, 207–213
63. Bragin, A. *et al.* (1995) Gamma (40–100 Hz) oscillation in the hippocampus of the behaving rat. *J. Neurosci.* 15, 47–60
64. Axmacher, N. *et al.* (2006) Memory formation by neuronal synchronization. *Brain Res. Rev.* 52, 170–182
65. Staudigl, T. and Hanslmayr, S. (2013) Theta oscillations at encoding mediate the context-dependent nature of human episodic memory. *Curr. Biol.* 23, 1101–1106
66. Tort, A.B.L. *et al.* (2009) Theta-gamma coupling increases during the learning of item-context associations. *Proc. Natl. Acad. Sci. U.S.A.* 106, 20942–20947
67. Belluscio, M.a. *et al.* (2012) Cross-frequency phase–phase coupling between theta and gamma oscillations in the hippocampus. *J. Neurosci.* 32, 423–435
68. Holz, E.M. *et al.* (2010) Theta–gamma phase synchronization during memory matching in visual working memory. *Neuroimage* 52, 326–335
69. Sauseng, P. *et al.* (2009) Brain oscillatory substrates of visual short-term memory capacity. *Curr. Biol.* 19, 1846–1852
70. Mazaheri, A. and Nieuwenhuis, I. (2009) Prestimulus alpha and mu activity predicts failure to inhibit motor responses. *Hum. Brain Mapp.* 30, 1781–1800
71. Mazaheri, A. *et al.* (2010) Functional disconnection of frontal cortex and visual cortex in attention-deficit/hyperactivity disorder. *Biol. Psychiatry* 67, 617–623
72. Shirvalkar, P.R. *et al.* (2010) Bidirectional changes to hippocampal theta–gamma comodulation predict memory for recent spatial episodes. *Proc. Natl. Acad. Sci. U.S.A.* 107, 7054–7059
73. Fries, P. (2009) Neuronal gamma-band synchronization as a fundamental process in cortical computation. *Annu. Rev. Neurosci.* 32, 209–224
74. Fries, P. *et al.* (2007) The gamma cycle. *Trends Neurosci.* 30, 309–316
75. Von Stein, A. and Sarnthein, J. (2000) Different frequencies for different scales of cortical integration: from local gamma to long range alpha/theta synchronization. *Int. J. Psychophysiol.* 38, 301–313
76. Buzsáki, G. and Draguhn, A. (2004) Neuronal oscillations in cortical networks. *Science* 304, 1926–1929
77. Bosman, C.A. *et al.* (2012) Attentional stimulus selection through selective synchronization between monkey visual areas. *Neuron* 75, 875–888
78. Doesburg, S.M. *et al.* (2009) Rhythms of consciousness: binocular rivalry reveals large-scale oscillatory network dynamics mediating visual perception. *PLoS ONE* 4, e6142
79. McGinn, R.J. and Valiante, T.a. (2014) Phase–amplitude coupling and interlaminar synchrony are correlated in human neocortex. *J. Neurosci.* 34, 15923–15930
80. Saalmann, Y.B. *et al.* (2012) The pulvinar regulates information transmission between cortical areas based on attention demands. *Science* 337, 753–756
81. Rosen, S. (1992) Temporal information in speech: acoustic, auditory and linguistic aspects. *Philos. Trans. R. Soc. Lond. B: Biol. Sci.* 336, 367–373
82. Schroeder, C.E. *et al.* (2010) Dynamics of active sensing and perceptual selection. *Curr. Opin. Neurobiol.* 20, 172–176
83. Pasley, B.N. *et al.* (2012) Reconstructing speech from human auditory cortex. *PLoS Biol.* 10, e1001251
84. Schroeder, C.E. *et al.* (2008) Neuronal oscillations and visual amplification of speech. *Trends Cogn. Sci.* 12, 106–113

relying on CFC, such as the purely sensory-driven gamma for visual stimulus de-multiplexing [28] or the deconnected theta–gamma control network for speech parsing [39].

85. Ghitza, O. (2011) Linking speech perception and neurophysiology: speech decoding guided by cascaded oscillators locked to the input rhythm. *Front. Psychol.* 2, 1–13
86. Morillon, B. *et al.* (2015) Predictive motor control of sensory dynamics in auditory active sensing. *Curr. Opin. Neurobiol.* 31C, 230–238
87. Arnal, L.H. and Giraud, A-L. (2012) Cortical oscillations and sensory predictions. *Trends Cogn. Sci.* 16, 390–398
88. Luo, H. and Poeppel, D. (2007) Phase patterns of neuronal responses reliably discriminate speech in human auditory cortex. *Neuron* 54, 1001–1010
89. Vanrullen, R. and Macdonald, J.S.P. (2012) Perceptual echoes at 10 Hz in the human brain. *Curr. Biol.* 22, 995–999
90. Kayser, C. *et al.* (2009) Spike-phase coding boosts and stabilizes information carried by spatial and temporal spike patterns. *Neuron* 61, 597–608
91. Panzeri, S. *et al.* (2014) Reading spike timing without a clock: intrinsic decoding of spike trains. *Philos. Trans. R. Soc. Lond. B: Biol. Sci.* 369, 20120467
92. Schroeder, C.E. and Lakatos, P. (2009) The gamma oscillation: master or slave? *Brain Topogr.* 22, 24–26
93. Gross, J. *et al.* (2013) Speech rhythms and multiplexed oscillatory sensory coding in the human brain. *PLoS Biol.* 11, e1001752
94. Burgess, N. and O'Keefe, J. (2011) Models of place and grid cell firing and theta rhythmicity. *Curr. Opin. Neurobiol.* 21, 734–744
95. Jensen, O. and Lisman, J. (1996) Novel lists of 7 ± 2 known items can be reliably stored an oscillatory short-term memory network: interaction with long-term memory. *Learn. Mem.* 3, 257–263
96. Akam, T.E. *et al.* (2012) Oscillatory dynamics in the hippocampus support dentate gyrus–CA3 coupling. *Nat. Neurosci.* 15, 763–768
97. Boerlin, M. *et al.* (2013) Predictive coding of dynamical variables in balanced spiking networks. *PLoS Comput. Biol.* 9, e1003258
98. Jensen, O. and Lisman, J.E. (1996) Theta/gamma networks with slow NMDA channels learn sequences and encode episodic memory: role of NMDA channels in recall. *Learn. Mem.* 3, 264–278
99. Akam, T.E. and Kullmann, D.M. (2012) Efficient 'communication through coherence' requires oscillations structured to minimize interference between signals. *PLoS Comput. Biol.* 8, e1002760
100. Gloveli, T. *et al.* (2005) Orthogonal arrangement of rhythm-generating microcircuits in the hippocampus. *Proc. Natl. Acad. Sci. U.S.A.* 102, 13295–13300
101. White, J.A. *et al.* (2000) Networks of interneurons with fast and slow-aminobutyric acid type A (GABAA) kinetics provide substrate for mixed gamma–theta rhythm. *Proc. Natl. Acad. Sci. U.S.A.* 97, 8128–8133
102. Kramer, M. and a *et al.* (2008) Rhythm generation through period concatenation in rat somatosensory cortex. *PLoS Comput. Biol.* 4, e1000169
103. Roopun, A.K. *et al.* (2008) Period concatenation underlies interactions between gamma and beta rhythms in neocortex. *Front. Cell. Neurosci.* 2, 1
104. Hansel, D. *et al.* (1995) Synchrony in excitatory neural networks. *Neural Comput.* 7, 307–337
105. Canavier, C.C. (2015) Phase-resetting as a tool of information transmission. *Curr. Opin. Neurobiol.* 31, 206–213
106. Gutkin, B.S. *et al.* (2005) Phase-response curves give the responses of neurons to transient inputs. *J. Neurophysiol.* 94, 1623–1635
107. Smeal, R.M. *et al.* (2010) Phase-response curves and synchronized neural networks. *Philos. Trans. R. Soc. Lond. B: Biol. Sci.* 365, 2407–2422
108. Canavier, C.C. *et al.* (2009) Phase resetting curves allow for simple and accurate prediction of robust N:1 phase locking for strongly coupled neural oscillators. *Biophys. J.* 97, 59–73
109. Pervouchine, D.D. *et al.* (2006) Low-dimensional maps encoding dynamics in entorhinal cortex and hippocampus. *Neural Comput.* 18, 2617–2650
110. Ermentrout, G. and Kopell, N. (1986) Parabolic bursting in an excitable system coupled with a slow oscillation. *SIAM J. Appl. Math.* 46, 233–253
111. Wilson, H.R. and Cowan, J.D. (1972) Excitatory and inhibitory interactions in localized populations of model neurons. *Biophys. J.* 12, 1–24
112. Krupa, M. and Szmolyan, P. (2001) Extending geometric sngular perturbation theory to nonhyperbolic points – fold and canard points in two dimensions. *SIAM J. Math. Anal.* 2, 23
113. Pillow, J.W. *et al.* (2008) Spatio-temporal correlations and visual signalling in a complete neuronal population. *Nature* 454, 995–999
114. Schneider, G. and Nikolić, D. (2006) Detection and assessment of near-zero delays in neuronal spiking activity. *J. Neurosci. Methods* 152, 97–106
115. Gerhard, F. *et al.* (2013) Successful reconstruction of a physiological circuit with known connectivity from spiking activity alone. *PLoS Comput. Biol.* 9, e1003138
116. Fontolan, L. *et al.* (2014) The contribution of frequency-specific activity to hierarchical information processing in human auditory cortices. *Nat. Commun.* 5, 4694